Characterization of Chain Orientation in Drawn Poly(*p*-phenylenevinylene) by ^2H Quadrupole Echo NMR Spectroscopy

Jeffrey H. Simpson, David M. Rice, and Frank E. Karasz*

Polymer Science and Engineering Department, University of Massachusetts, Amherst, Massachusetts 01003

Received March 2, 1991; Revised Manuscript Received September 27, 1991

ABSTRACT: Phenylene ring-deuterated poly(*p*-phenylenevinylene) films were prepared from water-cast films of the precursor polymer poly[(2,3,5,6-tetradeuterio-*p*-xylylidene)tetrahydrothiophenium chloride] and were heated and stretched to effect simultaneous orientation and elimination. ^2H quadrupole echo NMR spectra have been obtained from these films, aligned at an angle in the NMR magnetic field, for various draw ratios. The experimental data from ^2H spectra have been simulated with excellent agreement and thereby have yielded the chain orientation distribution in these films. ^2H spectra obtained at −58 °C are well simulated by an orientation distribution consisting of two Gaussian components, a well-oriented component with a width of 10° and a more poorly oriented component with a width of 30°. ^2H spectra obtained at 25 °C show a third component that is associated with well-oriented rings undergoing 180° rotational jumps about the 1,4-ring axis. The average tilt of the phenylene ring relative to the chain axis has been found to be 7.7°, close to but not exactly equal to the 9.2° predicted for a *trans*-stilbene-like structure. The difference can be attributed to chain disorder within crystallites or at domain boundaries.

Introduction

It has recently been reported that high-quality films of poly(*p*-phenylenevinylene) (PPV) can be prepared from water-cast films of a sulfonium salt precursor polymer.[1] These films show highly anisotropic conductivity when exposed to oxidative doping agents such as AsF_5.[2,3] The optical and tensile properties of these films are also of interest and have been discussed.[4-7]

In the present contribution the ^2H quadrupole echo NMR spectra of appropriately labeled PPV films have been obtained and analyzed to characterize the chain orientation distribution. Stretched PPV has been examined by a variety of methods, including infrared spectroscopy,[8] X-ray diffraction,[9] electron diffraction,[10,11] and electron microscopy.[12] Solid-state NMR methods, particularly ^2H quadrupole echo NMR, can provide new and independent data about PPV structure and morphology that may lead to a better theoretical understanding of PPV properties. ^2H NMR can also serve as a new method for monitoring the quality of processed PPV films.

As with any oriented, deuterated polymer, a stack of drawn PPV-d_4 films, aligned in the NMR magnetic field, will possess a ^2H spectral line shape that is dependent on the orientation distribution of C–D bonds in the film.[13,14] The ^2H NMR line shape of a specifically deuterated PPV can reveal the orientation distribution of the polymer chains relative to the stretching axis of the film and can indirectly provide information about the chain conformational disorder.

We have specifically incorporated deuterium in place of the phenylene ring protons of PPV and have characterized the ^2H NMR spectra of these oriented stretched films. The shape of the chain orientation distribution has been obtained through simulation of ^2H line shapes. ^2H NMR spectra also provide a measurement of the average tilt of the phenylene ring of PPV relative to the chain axis and provide some information about phenylene ring dynamics.

The utility of ^2H NMR for the study of an oriented polymer depends on the molecular geometry of the C–D bond relative to the chain. Because the C–D bonds of the phenylene ring are directed at 60° to the ring axis, the ^2H quadrupole splitting is particularly sensitive to small changes in chain orientation, and thus it has been possible to distinguish the spectra of well-oriented PPV from those of more poorly ordered chains. Previous studies of the deuterated phenyl or phenylene rings have been important in a variety of NMR studies of flexible chain polymers (cf. refs 15–17). The present results suggest the utility of the ^2H NMR study of the rigid phenylene rings for obtaining information about morphology in films and fibers containing rigid chains.

Experimental Section

Materials. Specifically labeled, ring-deuterated PPV precursor polymer poly[(2,3,5,6-tetradeuterio-*p*-xylylidene)tetrahydrothiophenium chloride) was prepared from the deuterated monomer (2,3,5,6-tetradeuterio-*p*-xylylene)bis(tetrahydrothiophenium) chloride according to a previously published procedure.[1] The procedure for the synthesis of the monomer also has been presented elsewhere.[18] Deuterated precursor films were cast from water and were either eliminated with stretching according to Gagnon et al.[1] or with the mechanical procedure of Machado et al.[19] to produce deuterated PPV-d_4 films (structure shown in Figure 1a). Films were eliminated at 250 °C under vacuum to complete elimination and had a thickness of 30 μm before stretching and, depending on the draw ratio, decreased to a thickness of 5–30 μm after stretching.

The specificity of labeling of the precursor polymer was confirmed by solution-state ^{13}C NMR with a Varian XL-300 NMR spectrometer in a H_2O/D_2O solution through observation of the proton-coupled spectrum. Ring deuteration was full (>95%), and methylene deuteration was undetectable (<5%). The specificity of labeling in the annealed films was confirmed by solid-state ^{13}C cross-polarization magic angle spinning (CP-MAS) NMR at 75 MHz with a Bruker MSL-300 NMR spectrometer by use of interrupted decoupling methods,[20] and by infrared spectroscopy.[21]

Methods. Sample Preparation. Powder samples of stretched and unstretched PPV-d_4 were obtained by cutting films into pieces with dimensions of approximately 1 mm^2. The pieces were packed in a 5-mm solids NMR tube (Wilmad 506-PP cut to a length of 3 cm).

NMR samples containing stacked films were prepared from both stretched and unstretched PPV-d_4. Films (10 mm wide)

* To whom correspondence should be addressed.

0024-9297/92/2225-2099$03.00/0

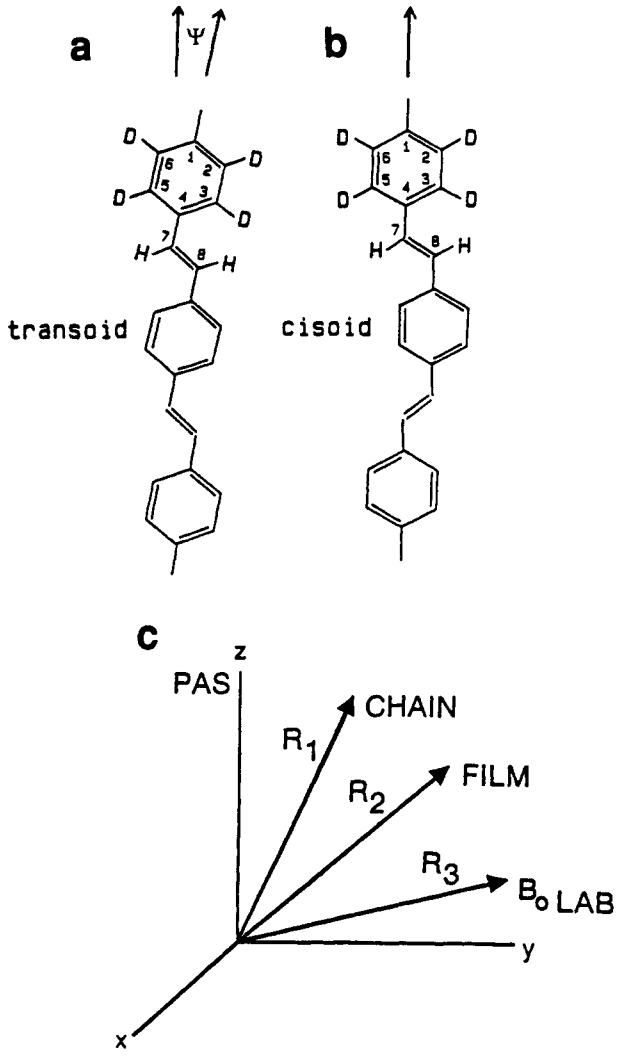

Figure 1. PPV structures showing coordinate axes and angles used to calculate the spectra of oriented films: (a) all-trans,transoid structure with stilbene-like geometry; (b) all-trans,cisoid structure. (c) The magnetic field vector $\mathbf{B}_0$ is aligned along the z axis of the laboratory frame (LAB) and is expressed in the C–D bond principal axis system (PAS) through three rotation matrix transformations. CHAIN, coordinate system fixed in the PPV chains; FILM, coordinate system fixed in the PPV film.

were folded, with folds perpendicular to the stretch axis, and inserted into a 5-mm-diameter rod containing a slot along its axis. Films were affixed to Kapton tape (CHR Industries) to preserve their structural integrity during folding. The folded edges were removed to leave an aligned stack of 5 mm × 10 mm films. The uncertainty of alignment was estimated at ±5° or less. The angle, Θ, between the stretching axis and the applied field was varied by rotating the film holder about its long axis in the NMR coil, an axis perpendicular to the NMR magnetic field.

^{2}H NMR Spectra. ^{2}H NMR spectra were obtained at 46 MHz in the 5-mm HP (high-power) probe of a Bruker MSL-300 instrument. Spectra were obtained with the two-pulse quadrupole echo NMR pulse sequence[22] with an eight-member phase cycle. The 90° pulse width was 2.3 μs, and the echo delay was 20 μs. The quadrupole echo was acquired, beginning 2 μs before its peak, with 2048 points at a rate of 5 MHz (2.5-MHz spectral width). The data were left-shifted to the echo peak and Fourier transformed into the observed spectrum with a Lorentzian line broadening of 2 kHz. The equilibrium recycle delay was determined by progressive saturation methods,[23] using the echo height; the equilibrium delay was 60 s at −58 °C and 20 s at 25 °C.

Theoretical Calculation of ^{2}H NMR Spectra. Theoretical ^{2}H NMR spectra were calculated with a specially written program that made use of the method of planar moments[13,14] to incorporate the effects of chain orientation as well as the method of Wittebort et al.[24] to incorporate the effects of phenylene ring dynamics and anisotropic quadrupole echo decay. The simulations were corrected for finite pulse width and finite probe bandwidth[23,25] as well as for natural line broadening.

Figure 1c describes the coordinate systems used to represent oriented PPV. The ^{2}H splitting, $\Delta\nu$, is a function of the normalized Cartesian coordinates of the magnetic field vector, $\mathbf{B}_0$, in the principal axis system (PAS; Figure 1c) of the C–D bond:[26]

$$\Delta\nu = \nu_{xx}\mathbf{B}_x^2 + \nu_{yy}\mathbf{B}_y^2 + \nu_{zz}\mathbf{B}_z^2 \quad (1)$$

where ν_{xx}, ν_{yy}, and ν_{zz} are the principal axis quadrupole splittings (tensor components) and $\mathbf{B}_x$, $\mathbf{B}_y$, and $\mathbf{B}_z$ are the normalized Cartesian coordinates of $\mathbf{B}_0$ in the principal axis system. The principal axes for the rigid lattice C–D bond are z (along the C–D bond) and y (perpendicular to the ring plane). The average principal axes for a phenylene ring undergoing fast rotational jumps are z (along the ring axis) and y (perpendicular to the ring plane). Equation 1, when expressed in spherical coordinates, has the form[13]

$$\Delta\nu = \Delta\nu_Q[(3\cos^2\theta - 1) - \eta\sin^2\theta\cos 2\phi] \quad (2)$$

where θ and ϕ are the spherical coordinates for $\mathbf{B}_0$; $\Delta\nu_Q = \nu_{zz}/2$, the quadrupolar splitting; and $\eta = (\nu_{yy} - \nu_{xx})/\nu_{zz}$, the asymmetry parameter, when the definitions of the principal axes are reordered such that $\nu_{xx} < \nu_{yy} < \nu_{zz}$. Values of $\Delta\nu_Q$ and η are included only for reference. Calculations are based upon eq 1, which includes no assumption about the relative magnitudes of ν_{xx} and ν_{yy}.

Values of $\mathbf{B}_x$, $\mathbf{B}_y$, and $\mathbf{B}_z$ in eq 1 were calculated by rotating the normalized value of $\mathbf{B}_0$ in the laboratory (LAB; Figure 1c) frame of reference (0, 0, 1) through three rotation matrix transformations, $\mathbf{R}_1$, $\mathbf{R}_2$, and $\mathbf{R}_3$, about axes of the C–D bond PAS coordinates (Figure 1c). The transformation $\mathbf{R}_1(\alpha_0,\beta_0,\gamma_0)$ relates the PAS coordinates to a coordinate system fixed in the PPV chain (CHAIN, z axis along the chain axis, y axis perpendicular to the ring plane, $\alpha_0 = 0°$, $\beta_0 = 60° \pm \Psi$, and $\gamma_0 = 0°$ or 180°). The value of Ψ, the phenylene ring tilt, is an experimental parameter and is determined by simulation.

The transformation $\mathbf{R}_2(\alpha,\beta,\gamma)$ relates the CHAIN coordinate system to a coordinate system fixed in the PPV film (FILM, z axis along the stretch axis, y axis in the film plane, $\alpha = 0$–360°, $\beta = 0$–180°, and $\gamma = 0$–360°). A powder average over α, β, and γ was performed by using an appropriate chain orientation distribution (eqs 3 and 4) as described in the Results and Discussion section. The transformation $\mathbf{R}_3(\Theta)$ relates the FILM coordinate system to the LAB coordinate system and the angle Θ is an experimental parameter, the angle between the stretching axis of the film and $\mathbf{B}_0$.

A value of the Hermans orientation function,[27] $f = \langle(3/2)\cos\beta - (1/2)\rangle$, was also calculated from the best-fit orientation distribution by numerical integration. The orientation functions obtained by NMR were compared with those previously obtained from the measurement of the infrared dichroism of similarly stretched, protonated films.[28]

Spectral Curve Fitting. Best-fit simulations were found through an automatic search of the parameters (an array of simulations) through minimization of least squares (χ^2), using specially written FORTRAN software. The uncertainties for each simulation parameter were determined both from statistical analysis and by visual inspection where necessary, as described in the Results and Discussion section. It is important to note that features that identify a particular model can be of low intensity and have only a marginal effect on χ^2. For the two-Gaussian model, described in the Results and Discussion section, the best-fit simulations were compared with those of a three-dimensional array of the adjustable parameters ($\Delta\beta$ for the narrow Gaussian component, P_{10}, and Ψ; see Table II for the definition of P_{10}). Deviation of $\Delta\beta$ for the broader component led to only minor changes in the position of singularities and the intensity of the outer edges of the spectra, as discussed in the Results and Discussion section, and did not affect the other parameters. The uncertainty for $\Delta\beta$ (±4°) for the narrow component was chosen on the basis of the three-peak structure in the center of the spectra (see Figure 4c). The uncertainty of Ψ (±0.5°) is illustrated by

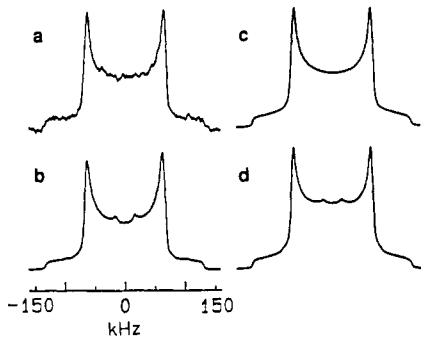

Figure 2. ^{2}H quadrupole echo NMR spectra of an unoriented PPV film (25 mg) at (a) −25 °C and (b) +25 °C and their simulations (c) $\Delta\nu_Q$ = 133 kHz and η = 0.03 and (d) the sum of $\Delta\nu_Q$ = 84 kHz and η = 0.63 plus $\Delta\nu_Q$ = 133 kHz and η = 0.03 in a 1 to 5.7 ratio.

Table I
Quadrupole Tensor Components (in kHz) for PPV-d_4 (Equation 1)[a]

structure	ν_{xx}	ν_{yy}	ν_{zz}
rigid lattice (−58 °C)	128	138	−266
rigid lattice (25 °C)	130	137	−266
ring flip (25 °C)	−168	137	32

[a] Tensor axes are defined in the Experimental Section. All values are ±1 kHz.

the calculated spectra of Figure 7, and the best value (7.7°) was determined from the width of the central component for search over Ψ based on χ^2 with acceptable values of $\Delta\beta$, as described in the Results and Discussion section.

For best-fit simulations, a functional relationship exists between $\Delta\beta$ (for a given Ψ) and the fraction with a 10° distribution, P_{10} (P_{30} = 1.0 − P_{10}), and this relationship affects the suitability of the two-Gaussian model. A systematic search over these parameters ($\Delta\beta$ = 6–24° and P_{10} = 0–1.0) showed a shallow (~50%) increase in χ^2 with increasing $\Delta\beta$ (and decreasing P_{10}) as well as the spectral features noted in the text. The quoted uncertainty for P_{10} (Table II) assumes the two-Gaussian model, $\Delta\beta$ = 10° and Ψ = 7.7°.

Results and Discussion

^{2}H Quadrupole Echo Powder Spectra of PPV-d_4. Figure 1a shows the structure of PPV-d_4, in which the phenylene ring protons have been replaced with deuterium. Figure 2 shows ^{2}H quadrupole echo powder spectra of unstretched films of this material, obtained at −25 °C (Figure 2a) and +25 °C (Figure 2b). The low-temperature spectrum in Figure 2a is a Pake doublet spectrum that results from a random orientation of deuterated phenylene rings, which undergo no observable molecular motion. For this spectrum, the measured quadrupole splitting, $\Delta\nu_Q$, is 133 ± 1 kHz and the asymmetry parameter, η, is 0.03 ± 0.01. A simulation is shown in Figure 2c, and the precise quadrupole tensor components (for eq 1) are shown in Table I. These values are similar to those obtained for other deuterated phenyl and phenylene rings.[15-17]

In contrast, the spectrum obtained at 25 °C (Figure 2b) can be deconvoluted into two components, a Pake doublet similar to Figure 2a and a second, narrower line shape. This second line shape is similar to that of phenylene rings which undergo fast 180° rotational jumps about the 1,4-ring axis (ring flips). The small doublet splitting of 32 kHz indicates the presence of the ring flip line shape, and this narrower line shape can be described with $\Delta\nu_Q$ = 84 ± 1 kHz and η = 0.63 ± 0.01. Tensor components for this line shape are shown in the last line of Table I. Figure 2d shows the calculated simulation, which verifies the deconvolution of Figure 2b. The ratio of the ring flip line shape to the Pake line shape is 1 to 5.7 ± 0.1, and this ratio shows that at ambient temperature approximately 15% of the phenylene rings in PPV films undergo 180° rotational jumps at a rate, k, greater than the quadrupole coupling frequency ($k > 1 \times 10^6$ s^{-1}).

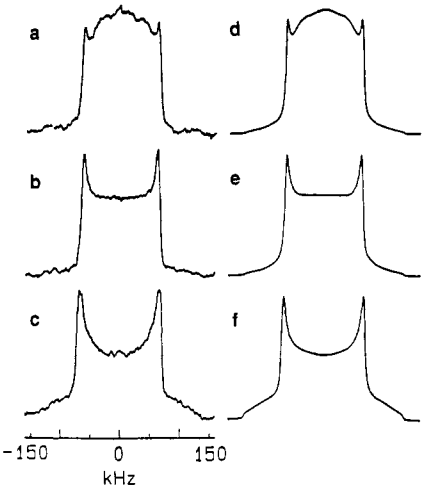

Figure 3. ^{2}H quadrupole echo NMR spectra of aligned, stretched films of PPV (10 mg) at −58 °C for (a) Θ = 0°, (b) Θ = 15°, and (c) Θ = 90°. Simulations with a narrow component (Ψ = 7.7° and $\Delta\beta$ = 10°) plus a broad component (Ψ = 7.7° and $\Delta\beta$ = 30°) in a 0.67 to 1 ratio for (d) Θ = 0°, (e) Θ = 15°, and (f) Θ = 90°. Quadrupole coupling parameters as in Figure 2c.

Data obtained from ^{13}C CP-MAS NMR spectra at ambient temperature have also shown the presence of ring flips (40%) and have shown that the percentage fast jump component increases with increasing temperature.[18] ^{2}H spectra obtained at higher temperatures also support this conclusion.[29] Such behavior has been shown to result from a temperature-dependent, continuous distribution of ring flip rates.

The intensity of the central region of the spectrum (between the peaks of the Pake doublet) is less than that in the simulation, and also the minimum between the peaks of the ring flip spectrum is deeper than that of the simulation. Both of these features are the result of anisotropic quadrupole echo relaxation,[30,31] and they indicate the presence of a population of phenylene rings with an intermediate ring flip rate. For the present investigation, we have chosen to keep the number of adjustable simulation parameters at a minimum. Low-temperature experimental conditions have been chosen to avoid the need to consider intermediate rate rotational jumps in simulations.

It is noted that ^{2}H powder spectra of PPV-d_4 films (which have been stretched and subsequently cut into pieces) are similar to the spectra of unstretched PPV. Stretching of PPV films has no effect on the quadrupole coupling parameters nor on the percentage of rings that undergo fast jumps at room temperature. If ring flips indicate regions of conformational disorder, stretching does not change the size of these regions.

^{2}H Quadrupole Echo Spectra of Aligned Films of Oriented PPV-d_4. Figure 3 shows the ^{2}H quadrupole echo spectra obtained from stacked PPV-d_4 films that have been aligned in the NMR magnetic field. These spectra were obtained at −58 °C, a temperature at which the effects of ring motion are absent. The spectrum of Figure 3a was obtained from a sample with the stretching axis aligned at Θ = 0° to the magnetic field axis $\mathbf{B}_0$. For parts b and c of Figure 3, the stretching axis was tilted at Θ = 15° and Θ = 90°, respectively. The spectrum of Figure 3a can be described as the sum of two components, a line

shape similar to a Pake doublet that causes the outer splitting and a narrower line shape that appears to have a flat top. The narrow component can be attributed to PPV crystallites that are well oriented with their c axes close to the stretching axis. The broader component can be attributed to more poorly oriented crystallites.

For phenylene ring-deuterated PPV, well-oriented and poorly oriented chains can be expected to show distinguishable spectral shapes and one can expect to obtain precise details about structure unique to the spectra of oriented phenylene rings. The C–D bonds of a phenylene ring are oriented at 60° relative to the 1,4-ring axis; and for a PPV chain oriented near the magnetic field direction (Figure 1a), the C–D bonds are at angles in the region of the magic angle, 54.7° to the field. At 54.7°, the quadrupole splitting is zero, and a well-oriented PPV chain should have a maximum intensity near zero frequency. In contrast, poorly oriented chains have a line shape resembling a Pake doublet, regardless of the geometry of the C–D bond. Near 54.7°, the quadrupole splitting is also very sensitive to changes in orientation, and the ^{2}H spectrum of PPV shows this sensitivity. For comparison, the C–D bonds of an *all-trans*-polymethylene chain are oriented 90° to the chain axis, and the quadrupole splitting for a perfectly oriented polymethylene chain is similar to that of the Pake doublet.[13] At an angle of 90°, the quadrupole splitting of a C–D bond is much less sensitive to small changes in orientation.

Characterization of ^{2}H Line Shapes for Oriented PPV. The spectra of Figure 3 are compared with calculated simulations and can provide quantitative data about the crystallite orientation and chain structure in stretched PPV films. The calculated ^{2}H spectra presented here are based on the current model for PPV structure as determined by X-ray and electron diffraction and by transmission electron microscopy.[9-12] In this model PPV films are thought to contain crystalline domains with an average crystallite size of 7 nm. The crystallinity is high, and the above techniques provide no evidence for separate amorphous domains, though some disorder must be present at domain boundaries. Tensile stress during elimination causes orientation of the crystallite c axes, and an orientation function of $f = 0.90$ or greater can be obtained for draw ratios less than $l/l_0 = 10$.[28]

Individual PPV chains are assumed to be present in the all-trans configuration (Figure 1a) with the chain axis oriented close to the crystallite c axis. The PPV chain is assumed to be planar and assumed to have a structure similar to *trans*-stilbene; all vinylene groups are assumed to be parallel to one another in a transoid structure.[10] For this structure (Figure 1a), the 1,4 axes of each phenylene ring should also be parallel to one another. The stilbene geometry predicts an angle of 9.2° between the phenylene ring axis and the crystallite c axis. We refer to this angle as the phenylene ring tilt and represent it with the symbol Ψ.

Figure 4a shows the calculated ^{2}H line shape that is expected for a nearly perfectly oriented PPV film (crystallite misalignment of ±1°) with its stretch axis aligned parallel to the magnetic field. The line shape consists of two quadrupole doublets that are associated with C–D bonds oriented at each of two angles to the chain axis (Figure 1a); the deuterons of the phenylene ring are oriented at 60° to the 1,4-ring axis. It can be seen from Figure 1a that deuterons at carbons C3 and C6 are oriented at an angle less than 60° to the chain axis as a result of the tilt of the phenylene ring. The inner splitting can be attributed to the deuterons at C2 and C5, which are

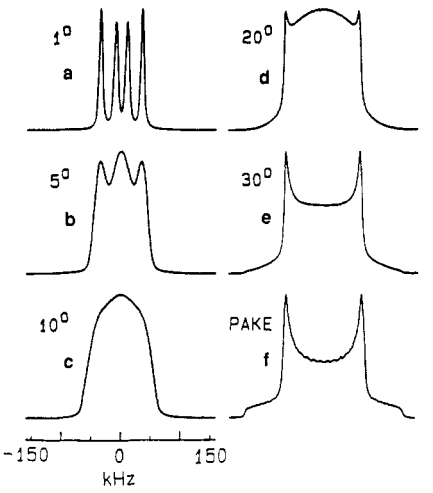

Figure 4. Calculated ^{2}H NMR spectra for several Gaussian orientation distributions with width $\Delta\beta$ as indicated (1°, 5°, 10°, 20°, 30°, PAKE) $\Psi = 7.7°$, for oriented PPV films aligned with their stretch axis parallel to the magnetic field; $\Theta = 0°$.

oriented at an angle greater than 60° to the chain.

Parts b–e of Figure 4 show the calculated line shapes expected for several other distributions of crystallite orientation of greater width. For the calculation of these line shapes, the distribution of crystallite c axes was assumed to be a Gaussian function of the angle between the chain axis and the stretching axis as shown in eq 3, where

$$P(\alpha,\beta,\gamma) = [P(\beta=0)]e^{-(\beta/\Delta\beta)^2} \quad (3)$$

the angular width $\Delta\beta$ is defined as the angle corresponding to $P(\alpha,\beta,\gamma) = P(0)e^{-1}$. The angles α, β, and γ are defined in the Experimental Section. Figure 4f is the Pake doublet line shape resulting from a completely isotropic distribution of crystallites.

The two components of Figure 3a can each be associated with a line shape similar to one in Figure 4 (calculated from a Gaussian crystallite distribution), and the spectrum can be simulated with a sum of these two line shapes. The crystallite orientation distribution can therefore be represented empirically by a sum of two Gaussian functions with different widths. The spectrum obtained at the $\Theta = 0°$ orientation can be deconvoluted into a narrow line shape similar to Figure 4c, $\Delta\beta = 10°$, and a doublet similar to Figure 4e, $\Delta\beta = 30°$. The two line shapes have intensities in a ratio of 1 to 0.67 ± 0.01. A Hermans orientation function, $f = 0.85$, has been calculated for the two-component distribution. This value is consistent with that obtained from infrared dichroism data.[8,28]

The spectra of the films that have been rotated at angles of $\Theta = 15°$ (Figure 3b) and $\Theta = 90°$ (Figure 3c) are consistent with the two-component Gaussian distribution. The overall change in spectral shape with the alignment angle, Θ, is reproduced in simulations (Figure 3d–f). Observation of the expected change in the spectral shape with film rotation verifies that the spectrum of Figure 3a is indeed the result of oriented chains.

Two features of the spectra and simulations of rotated films should be noted. First, the spectra at all orientations lack the step-function edges that are usually associated with the Pake doublet spectrum of an isotropic distribution. The lack of such edges distinguishes the spectrum of a 30° distribution (Figure 4e) from that of an isotropic distribution (Figure 4f) and suggests that there are no unoriented segments within these films. Second, the apparent frequency difference between the peaks of Figure 3c ($\Theta = 90°$) is about 3% greater than that between the

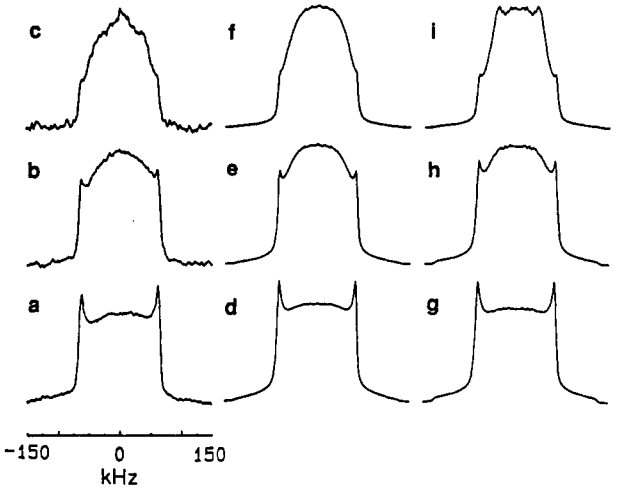

Figure 5. ^2H quadrupole echo NMR spectra of stretched films of PPV aligned at $\Theta = 0°$ for several different draw ratios (a–c) and their simulations based on a sum of Gaussian distributions (d–f) or on the pseudoaffine distribution (g–i). Draw ratios: (a) $l/l_0 = 2.0$; (b) $l/l_0 = 3.0$; (c) $l/l_0 = 6.0$. Simulations based on a sum of Gaussian distributions: (d) $P_{10} = 0.16$; (e) $P_{10} = 0.42$; (f) $P_{10} = 0.66$ (see Table II). Simulations based on the pseudoaffine distribution: (g) $\lambda = 2.4$; (h) $\lambda = 3.2$; (i) $\lambda = 5.1$ (see Table II).

peaks of Figure 3a ($\Theta = 0°$). Also, this difference is 3% greater than that of the powder spectrum of Figure 2a. Simulations reproduce this change, and the change in splitting can be attributed to the effect of the axial asymmetry of the C–D bond ($\eta = 0.03$) on the line shape of the $\Theta = 90°$ orientation. The change cannot be attributed to a change in the quadrupole coupling tensor components with stretching because stretching does not affect the quadrupole splitting as measured from the powder spectrum. The 3% change in splitting also distinguishes the spectrum of the 30° distribution from that of the isotropic distribution and establishes that all PPV segments in these samples are oriented. If a substantial population of unoriented PPV were present, a second narrower splitting would be present in Figure 3c.

The change also establishes that $|\nu_{yy}|$ (the quadrupole coupling tensor component perpendicular to the ring) is greater than $|\nu_{xx}|$. If the opposite were true, the quadrupole splitting of Figure 3c would be 3% smaller than the powder splitting. It is important to note that this relationship between ν_{yy} and ν_{xx} is also necessary for the simulation of the 32-kHz splitting of the ring flip component of Figure 2b and the asymmetry parameter of $\eta = 0.63$. The consistency of these two details supports the assumption that the ν_{zz} component of the quadrupole coupling tensor coincides with the C–D bond direction, and deviation of the ring flip asymmetry parameter from 0.60 can be attributed entirely to the rigid lattice asymmetry parameter of the C–D bond. The relative magnitudes of ν_{xx} and ν_{yy} are also consistent with the assignment of chemical shift tensor axes of aromatic rings.[32]

Dependence of the Orientation on Draw Ratio. Parts a–c of Figure 5 show three ^2H spectra of PPV films stretched to various draw ratios ($l/l_0 = 2.0$, 3.0, and 6.0). Increasing the draw ratio decreases the intensity at outer frequencies of the spectrum and increases the intensity of the central component. These spectra have been simulated with the distribution used for Figure 3 (a sum of two Gaussian functions with $\Delta\beta = 10°$ and $\Delta\beta = 30°$), and this distribution provides a good fit, as shown in parts d–f of Figure 5. The two Gaussian functions have been weighted differently for each draw ratio, and the fractions P_{10} (fraction with $\Delta\beta = 10°$) and P_{30} ($P_{30} = 1 - P_{10}$) are shown

Table II
Simulation Parameters and Orientation Functions for the Spectra of Stretched PPV-d_4 at Three Draw Ratios

l/l_0	P_{10}[a] (±0.02)	P_{30}[a] (±0.02)	f_{Gauss}[b]	λ[c] (±0.1)	f_{Kratky}[b]	f_{IR}[b]
2.0	0.16	0.84	0.72	2.4	0.55	0.72
3.0	0.42	0.58	0.79	3.2	0.68	0.84
6.0	0.66	0.34	0.86	5.1	0.81	0.92

[a] P_{10} is the fraction with $\Delta\beta = 10°$. $P_{30} = 1 - P_{10}$. [b] f_{Gauss}, Hermans orientation function; f_{IR}, orientation function obtained from the infrared dichroic ratios of similarly stretched, protonated PPV films with the relevant draw ratio; f_{Kratky}, calculated orientation function, from the Kratky distribution. [c] λ, defined in eq 4.

for each draw ratio in Table II (columns 2 and 3). It should be noted that, within the precision of these spectra, there is no need to alter the value of $\Delta\beta$ or add extra Gaussian components. The draw ratio dependence of ^2H spectra can be fit by changing one parameter, P_{10}.

An alternative fitting procedure based on a single Gaussian width, $\Delta\beta_0$, might be employed. The spectrum of Figure 3a is similar to the $\Delta\beta = 20°$ simulation of Figure 4d. However, note that the central component of the experimental spectrum (Figure 3a) is narrower than the central component in Figure 4f. This difference leads to marginally greater values of χ^2. Simulation with a narrower width, to fit the center of the spectrum, reduces the intensity of the Pake singularities and causes the need for the second component with a broader Gaussian ($\Delta\beta = 30°$). The implication of a two-component distribution is that crystallite orientation at higher angles is more probable than can be described by a single Gaussian. It should be noted that a single Gaussian function has no particular theoretical justification as a crystallite orientation distribution for PPV films, and accepted models (such as the pseudoaffine model[33]) predict a greater intensity at high angles. Two Gaussians are used in preference to the single Gaussian in order to quantify these differences at high angles.

Table II, column 4, also shows the value of the Hermans orientation function, f_{Gauss}, derived from each distribution. Column 7 contains the values of the orientation function, f_{IR}, obtained from the infrared dichroic ratios of similarly stretched, protonated PPV films with the same draw ratio, l/l_0. For the lowest draw ratio, the orientation functions obtained from NMR and infrared spectroscopy are in good agreement. For the higher draw ratios, $f_{Gauss} < f_{IR}$ and the difference can be attributed to uncertainty of film alignment. Infrared data can be obtained from a single film, whereas NMR data must obtained from stacked films with a corresponding uncertainty of alignment. NMR measurements do not represent the narrowest components of the orientation distribution.

It is useful to compare the experimental spectra of Figure 5 with those which would result from the pseudoaffine or Kratky model.[33] The pseudoaffine model provides a theoretical relationship between the orientation distribution and the experimental draw ratio and has been used previously to characterize PPV orientation data obtained from the infrared dichroic ratio. It has been shown that PPV orientation is better than that predicted by the pseudoaffine model.[8,28] In particular, the experimental orientation function, f_{IR}, obtained from the infrared dichroic ratio, is greater than that obtained by integration of the Kratky distribution when $l/l_0 = \lambda$. The Kratky distribution is shown in eq 4, where α, β, and γ have definitions similar to that described in eq 3 and the Experimental Section. The single parameter λ is compared with the experimental draw ratio. Simulations of the experimental spectra with this distribution are shown in

$$P(\alpha,\beta,\gamma) = \frac{\lambda^{3/4}}{(\lambda^{3/2}\sin^2\beta + \lambda^{-3/2}\cos^2\beta)^{3/2}} \quad (4)$$

parts g–i of Figure 5. The best-fit values of λ for each simulation with the Kratky distribution are shown in Table II, column 5, along with the calculated orientation function, f_{Kratky}, in column 6. For the draw ratios $l/l_0 = 2.0$ and 3.0, the Kratky distribution provides a reasonable fit of the experimental spectra, especially in the center of the spectrum. However, there are subtle differences between the high-frequency edges of the experimental spectra and Kratky simulations. The best-fit simulations with the Kratky distribution include step-function edges, which are not evident in experimental spectra. Also, the orientation functions derived from the Kratky distribution, f_{Kratky}, are smaller than those determined from the best-fit Gaussian distribution, f_{Gauss}. The values of f_{Kratky} are also less than f_{IR}, the experimental orientation function determined from infrared dichroism.

For the draw ratio $l/l_0 = 6.0$, the Kratky simulation (Figure 5i) provides a reasonable fit to the edges of the spectrum, and f_{Gauss} and f_{Kratky} are closer in magnitude. However, the center of the simulation of Figure 5i contains some structure that is not evident in the experimental spectrum. The additional structure can be attributed to a fraction of chains whose orientation angle is less than 10°. The spectrum of Figure 5c does not contain this structure; however, these very highly oriented chains should be unobservable due to the uncertainty of stacked film alignment.

^{2}H NMR data suggest why the orientation functions determined from the infrared dichroic ratio are greater than those predicted by the pseudoaffine model. The step-function edges of the Kratky simulations result from very poorly oriented chains (at close to 90° to the stretching axis). The pseudoaffine model overestimates the number of these chains, and this overestimation yields a substantially lower orientation function and dichroic ratio. The fraction of chains in the overestimation can be determined from the integrals of the spectra and simulations; and it should be noted that only a small fraction of chains are involved. These chains, however, substantially lower the orientation function, because they are oriented at close to 90° to the stretching axis. For the low draw ratios, the pseudoaffine model provides a good fit to the orientation distribution of the majority of chains with low orientation angle, and it can be seen in Table II that the values of λ obtained by simulation (neglecting the difference at the edges) are similar to the experimental draw ratios. At high draw ratios, the pseudoaffine distribution properly describes the chains with large orientation angle, but overestimates the fraction of chains with alignment better than $\beta = 10°$.

Figures 3 and 5 show that, with the above qualifications, the orientation distribution for most of the segments of stretched PPV could readily result from the assumptions of the pseudoaffine model. It should be emphasized that the poorly oriented component of the empirical distribution does not necessarily represent a distinguishable domain and that segments in both crystallites and boundary domains have orientations at least as good or better than that predicted by the pseudoaffine model.

The spectra of Figures 3 and 5 do not provide information about the relationship between domain structure and orientation. Dark-field transmission electron microscopy (TEM) pictures have suggested, however, that boundary domains may contribute preferentially to the broad component of the orientation distribution.[12] TEM

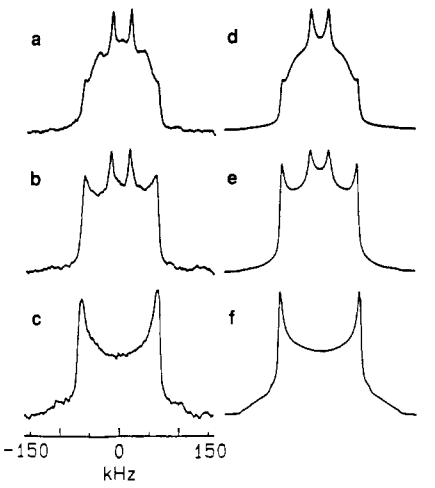

Figure 6. ^{2}H quadrupole echo NMR spectra of aligned, stretched films of PPV (10 mg) at 25 °C for (a) $\Theta = 0°$, (b) $\Theta = 15°$, and (c) $\Theta = 90°$. Simulations based on Gaussian distributions with a narrow component ($\Psi = 7.7°$ and $\Delta\beta = 10°$) plus a broad component ($\Psi = 7.7°$ and $\Delta\beta = 30°$) in a 1.33 to 1 ratio, with static rings and flipping rings in a 9 to 1 ratio for (d) $\Theta = 0°$, (e) $\Theta = 15°$, and (f) $\Theta = 90°$. Quadrupole coupling parameters as in Figure 2d.

data obtained from a partially oriented film similar to that of Figure 3 do not show a significant number of crystallites at angles greater than 10° from the stretching axis.[34] These data suggest that the more poorly oriented segments observed by NMR may exist within boundary domains where they are not observable by TEM.

^{2}H Quadrupole Echo Spectra of Oriented PPV-d_4 at 25 °C. Figure 6 shows the ^{2}H spectra of an oriented PPV film obtained at 25 °C. The spectrum of Figure 6a, aligned at $\Theta = 0°$ to the field, shows the presence of the two components of Figure 3a but also contains an additional doublet with a quadrupole splitting of about 25% of the Pake doublet splitting. This doublet can be attributed to the phenylene rings of well-oriented crystallites that undergo rapid 180° rotational jumps. A similar spectrum has also been reported for the phenylene rings of an oriented side-chain liquid-crystalline polyacrylate, as shown by Pschorn et al.,[14] and our calculations show that it should also be expected for PPV. Figure 6d shows a simulation of Figure 6a that results from an orientation distribution with Gaussian components similar to those of Figure 3, except that 10% of the phenylene rings are represented by a fast jump line shape. Rotation of the film axis away from the field axis (increasing Θ) causes the oriented ring flip doublet to disappear (parts b and c of Figure 6). This disappearance is expected and has been reproduced in simulations (parts e and f of Figure 6).

For semicrystalline polymers containing phenylene rings, it has been noted that fast ring flips occur principally in amorphous or crystallite boundary domains[35] (including two related structures, poly(*p*-phenylene)[36] and polyaniline[37]). However, the observation of a well-oriented ring flip component for PPV indicates that within the experimental precision of these spectra there is no correlation between the ring flip motion and orientation. Ring flips must be found in both well-oriented and poorly oriented domains. If, as TEM data suggest, the well-oriented domains are principally crystallites and the poorly oriented domains are principally boundary domains, then one must conclude that ring flips are present in crystallites as well as boundary domains. The temperature dependence of ^{2}H spectra also supports this conclusion.[29]

These spectra do not rule out a more subtle relationship between ring flip motion and orientation. The powder

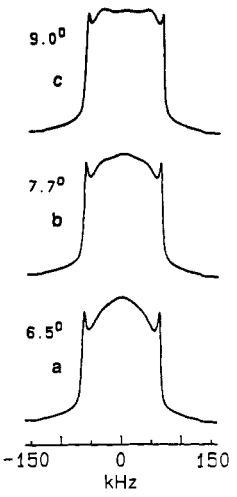

Figure 7. Calculated ^2H spectra for three phenylene ring tilt angles, Ψ: (a) 6.5°; (b) 7.7°; (c) 9.0°. Other parameters as in Figure 3d.

spectrum of Figure 2b indicates a 15% fast jump component whereas Figure 6 indicates a 10% component. Also Figure 5 indicates a smaller percentage for the $\Delta\beta = 30°$ distribution than Figure 3. More precise simulation of the spectra of Figure 5 is possible, but this simulation would also require consideration of anisotropic quadrupole echo decay and additional knowledge of the ring flip rate distribution. With the additional parameters, lineshape simulation would not yield a clear answer, although two new two-dimensional NMR methods could potentially provide additional data.[38,39] Stretched PPV films with their good orientation provide an excellent opportunity to study the mechanism of the ring flip motion and its relationship to orientation order.

Determination of the Phenylene Ring Tilt Angle. Simulation of the spectra of Figure 3 allows experimental determination of the angle of phenylene ring tilt, Ψ, relative to the chain axis. Figure 7 shows a set of simulations for Figure 3a for three tilt angles $\Psi = 6.5°$, 7.7°, and 9.0°. A tilt angle of 7.7 ± 0.5° has been found to best fit the experimental width of the central component of Figure 3a. Also, the use of a 7.7° tilt angle leads to values of the orientation function (Table II) consistent with those obtained from infrared dichroism measurements. The experimental value is close to the value of 9.2° predicted for PPV with a trans,transoid configuration and a stilbene geometry, and the observation of phenylene ring tilt supports the assumption that PPV chains are well organized in this structure. The phenylene ring tilt has also been obtained from the measurement of infrared dichroism of protonated films ($\Psi = 9.0°$).[8,28]

NMR line shapes clearly distinguish a tilt angle of 7.7° from an angle of 9.2°. The width of the central component of Figure 7c is greater than that of Figure 7b and greater than the experimental width. Such a precise measurement of tilt is possible because the C–D bonds of well-oriented chains are close to the magic angle (54.7°), where the spectral line shape is very sensitive to angle. Also, the orientation width ($\Delta\beta = 10°$) is of the same magnitude as the tilt angle ($\Psi = 7.7°$), so the effects of both parameters are equally evident in simulations. In particular, the tilt angle affects the frequency splitting of the deuterons at C3 and C6. For an orientation distribution with a finite width, the two doublets are not distinguished and the result is apparent as a change in the overall width of the central component of the line shape. For a larger tilt angle, the spectrum is broader with a more rectangular shape, and for a small tilt angle the spectrum is narrower and has a peak.

The 1.5° deviation can be attributed to disorder within the PPV structure, either within crystallites or at domain boundaries. To obtain a planar, trans,transoid PPV structure with a 7.7° tilt angle, the PPV segmental length would have to be stretched by 0.1 nm or the vinylene bond length would have to be decreased by 0.02 nm. Such structures would have chemically unlikely bond lengths and angles and would be in conflict with diffraction data. The deviation could, however, be explained with a nonplanar PPV structure containing static rotational disorder about the phenylene–vinylene bonds. The planar PPV structure has a maximum value of phenylene ring tilt. Small-angle rotation about phenylene–vinylene bonds would reduce the angle between the C–D bonds of C3 and C6 and the crystallite c axis and lead to a smaller apparent tilt angle. Recently, Winokur and co-workers have obtained new, precise X-ray data that suggest that the dihedral angle between the phenylene and vinylene groups in crystallites is ~20°. Such a nonplanar PPV structure could result in the observed phenylene ring tilt.[40]

Alternatively, the experimental tilt angle could result from a planar chain containing one or more segments in a trans,cisoid structure (Figure 1b). In this structure a single vinylene group is aligned in an opposite direction from its neighbors; and for a structure with an alternating cisoid configuration, the phenylene ring tilt angle is zero. The 7.7° experimental tilt angle might be attributed to 1 cisoid configuration in about 12 segments. It should be noted that 12 PPV segments would easily span the crystallite length of 7 nm. A cisoid defect at the crystallite boundary would tilt the PPV chain about an axis perpendicular to its plane and reduce the phenylene ring tilt angle relative to the crystallite c axis.

Conclusions

^2H NMR spectra have provided new details about crystalline structure and chain disorder within stretched PPV films. NMR data confirm the results of diffraction experiments which show that the PPV chain has a high crystallinity. ^2H spectra show independently that the phenylene ring is tilted relative to the crystallite c axis, as expected for segments with a trans,transoid structure and a stilbene geometry. A 1.5° discrepancy between the predicted and experimental tilt has been attributed to the presence of chain disorder at crystallite boundaries or to small-angle rotational disorder about the phenylene–vinylene bonds at each segment.

NMR data show that PPV films are highly oriented by stretching, and the orientation function determined by NMR is similar to that obtained from the infrared dichroic ratio. NMR spectra provide information about the shape of the orientation distribution and show that the orientation distribution for most segments can be adequately described by the pseudoaffine model. However, stretched PPV films possess fewer chains at 90° to the stretching axis than predicted by the pseudoaffine model. Although the fraction of chains involved is small, this difference can explain the higher orientation functions obtained for PPV from the infrared dichroic ratio.

NMR spectra show that at room temperature a fraction of PPV segments contain phenylene rings that undergo 180° rotational jumps. This jump motion is also present in stretched samples, and the existence of a well-oriented jump spectrum suggests that this motion can occur within PPV crystallites as well as boundary domains. Ring flip motion in both crystalline and boundary domains of a

polymer is rare. Although ring flip motion has been observed in some small molecular weight crystalline materials,[17,23,31] we suggest that for PPV the motion is related to the disorder within the crystalline structure. Stretched PPV films, with their good orientation, provide an excellent opportunity to study the ring flip mechanism and its relationship to orientation order.

Acknowledgment. We thank Drs. M. A. Masse and J. M. Machado for helpful discussions and Professor H. W. Spiess for valuable comments about Figure 6a. Dr. Masse also provided FTIR data and TEM data for deuterated films. This work was supported by AFOSR Grant No. 90-0010.

References and Notes

(1) Gagnon, D. R.; Capistran, J. D.; Karasz, F. E.; Lenz, R. W.; Antoun, S. *Polymer* **1987**, *28*, 567.
(2) Gagnon, D. R.; Capistran, J. D.; Karasz, F. E.; Lenz, R. W. *Polym. Bull.* **1984**, *12*, 293.
(3) Murase, I.; Ohnishi, T.; Noguchi, T.; Hirooka, M. *Polym. Commun.* **1984**, *25*, 327.
(4) Obrzut, J.; Karasz, F. E. *J. Chem. Phys.* **1987**, *87*, 6178.
(5) Obrzut, J.; Karasz, F. E. *Nonlinear Optical and Electroactive Polymers*; Prasad, P. N.; Ulrich, D. R., Eds.; Plenum: New York, 1988; p 273.
(6) Singh, B. P.; Prasad, P. N.; Karasz, F. E. *Polymer* **1988**, *29*, 1940.
(7) Machado, J. M.; Karasz, F. E.; Lenz, R. W. *Polymer* **1988**, *29*, 1412.
(8) Bradley, D. D. C.; Friend, R. H.; Lindenberger, H.; Roth, S. *Polymer* **1986**, *27*, 1709.
(9) Bradley, D. D. C. *J. Phys. D: Appl. Phys.* **1987**, *20*, 1389.
(10) Granier, T.; Thomas, E. L.; Gagnon, D. R.; Karasz, F. E.; Lenz, R. W. *J. Polym. Sci., Part B: Polym. Phys.* **1986**, *24*, 2793.
(11) Granier, T.; Thomas, E. L.; Karasz, F. E. *J. Polym. Sci., Part B: Polym. Phys.* **1989**, *27*, 469.
(12) Masse, M. A.; Martin, D. C.; Thomas, E. L.; Karasz, F. E.; Petermann, J. H. *J. Mater. Sci.* **1989**, *25*, 311.
(13) Spiess, H. W. In *Developments in Oriented Polymers. 1*; Ward, I. M., Ed.; Applied Science Publishers: Essex, U.K., 1982.
(14) Pschorn, V.; Spiess, H. W.; Hisgen, B.; Ringsdorf, H. *Makromol. Chem.* **1986**, *187*, 2711.
(15) Choli, A. L.; Dumais, J. J.; Engle, A. K.; Jelinski, L. W. *Macromolecules* **1984**, *17*, 2399.
(16) Spiess, H. W. *Adv. Polym. Sci.* **1985**, *66*, 23.
(17) Griffin, R. G.; Beshah, K.; Ebelhauser, R.; Huang, T. H.; Olejniczak, E. T.; Rice, D. M.; Siminovitch, D. J.; Wittebort, R. J. In *The Time Domain in Surface and Structural Dynamics*; Long, G. J., Grandjean, F., Eds.; Kluwer: New York, 1988; p 81.
(18) Simpson, J. H.; Egger, N.; Masse, M. A.; Rice, D. M.; Karasz, F. E. *J. Polym. Sci., Part B: Polym. Phys.* **1990**, *28*, 1859.
(19) Machado, J. M.; Karasz, F. E.; Kovar, R. F.; Burnett, J. M.; Druy, M. A. *New Polym. Mater.* **1989**, *1*, 189.
(20) Opella, S. J.; Frey, M. H. *J. Am. Chem. Soc.* **1979**, *101*, 5854.
(21) Liang, W. B.; Rice, D. M.; Karasz, F. E. *Polym. Commun.*, in press.
(22) Davis, J. H.; Jeffrey, K. R.; Bloom, M.; Valic, M. I.; Higgs, T. P. *Chem. Phys. Lett.* **1976**, *42*, 390.
(23) Rice, D. M.; Meinwald, Y. C.; Scheraga, H. A.; Griffin, R. G. *J. Am. Chem. Soc.* **1987**, *109*, 1636.
(24) Wittebort, R. J.; Olejniczak, E. T.; Griffin, R. G. *J. Chem. Phys.* **1987**, *86*, 5411.
(25) Bloom, M.; Davis, J. H.; Valic, M. I. *Can. J. Phys.* **1981**, *58*, 1510.
(26) Mehring, M. *High Resolution NMR of Solids*, 2nd ed.; Springer-Verlag: Berlin, 1983; p 26.
(27) Folkes, M. J.; Ward, I. M. In *Structure and Properties of Oriented Polymers*; Ward, I. M., Ed.; John Wiley & Sons: New York, 1975; p 219.
(28) Machado, J. M. Ph.D. Thesis, University of Massachusetts, Amherst, MA, 1988.
(29) Simpson, J. H.; Rice, D. M.; Karasz, F. E. *J. Polym. Sci., Part B: Polym. Phys.* **1992**, *30*, 11.
(30) Spiess, H. W.; Sillescu, H. J. *J. Magn. Reson.* **1981**, *42*, 381.
(31) Rice, D. M.; Wittebort, R. J.; Griffin, R. G.; Meirovitch, E.; Stimson, E. R.; Meinwald, Y. C.; Freed, J. H.; Scheraga, H. A. *J. Am. Chem. Soc.* **1981**, *103*, 7707.
(32) Mehring, M. *High Resolution NMR of Solids*, 2nd ed.; Springer-Verlag: Berlin, 1983; p 185.
(33) Hadley, D. W.; Ward, I. M. *Structure and Properties of Oriented Polymers*; Ward, I. M., Ed.; John Wiley & Sons: New York, 1975; p 264.
(34) Masse, M. A.; Karasz, F. E., unpublished data.
(35) Jelinski, L. W. In *High Resolution NMR Spectroscopy of Synthetic Polymers in Bulk*; Komoroski, R. A., Ed.; VCH: Weinheim, FRG, 1986; p 335.
(36) Dumais, J. J.; Jelinski, L. W.; Galvin, M. E.; Dybowski, C.; Brown, C. E.; Kovacic, P. *Macromolecules* **1989**, *22*, 612.
(37) Kaplan, S.; Conwell, E. M.; Richter, A. F.; MacDiarmid, A. G. *Macromolecules* **1989**, *22*, 1669.
(38) Schmidt, C.; Bluemich, B.; Spiess, H. W. *J. Magn. Reson.* **1988**, *79*, 269.
(39) Yang, Y.; Hagemeyer, A.; Spiess, H. W. *Macromolecules* **1989**, *22*, 1004.
(40) Chen, D.; Winokur, M. J.; Masse, M. A.; Karasz, F. E. *Polymer*, in press.

Registry No. PPV (SRU), 26009-24-5; poly[(*p*-xylylidene)-tetrahydrothiophenium chloride], 135372-29-1.